Antitumor activity of ginsenoside Rg3 in melanoma through downregulation of the ERK and Akt pathways

LINGBIN MENG[1,2], RUI JI[3], XIAOMING DONG[4], XIAOCHUN XU[5], YING XIN[4] and XIN JIANG[1]

[1]Department of Radiation Oncology, The First Hospital of Jilin University, Changchun, Jilin 130021, P.R. China; [2]Department of Internal Medicine, Florida Hospital, Orlando, FL 32803; [3]Department of Biology, Valencia College, Orlando, FL 32825, USA; [4]Key Laboratory of Pathobiology, Ministry of Education, Jilin University, Changchun, Jilin 130021, P.R. China; [5]Department of Clinical Cancer Prevention, The University of Texas M.D. Anderson Cancer Center, Houston, TX 77030, USA

Received January 16, 2019; Accepted April 2, 2019

DOI: 10.3892/ijo.2019.4787

Abstract. Advanced metastatic melanoma is a malignant tumor for which there is currently no effective treatment due to resistance development. Ginsenoside Rg3, a saponin component extracted from ginseng roots, has been shown to reduce melanoma cell proliferation by decreasing histone deacetylase 3 and increasing p53 acetylation. The availability of data on the role of Rg3 in melanoma is currently extremely limited. The aim of the present study was to further investigate the effects of Rg3 on B16 melanoma cells and the underlying molecular events. The findings demonstrated that Rg3 suppressed the proliferation and DNA synthesis of B16 cells. Rg3 exposure induced tumor cell cycle arrest at the S phase and reduced the expression of proliferating cell nuclear antigen (PCNA). Rg3 treatment also decreased metastasis of B16 cells *in vitro* and *in vivo*. The results indicated that this reduction was due to downregulation of matrix metalloproteinase (MMP)-2 and MMP-9. Moreover, Rg3 inhibited melanoma-induced angiogenesis, most likely by downregulating vascular endothelial growth factor (VEGF) in B16 cells. Rg3 exposure decreased the expression of VEGF in B16 cells and the VEGF downregulation further suppressed angiogenesis by attenuating the proliferation and migration of vascular endothelial cells. Finally, the western blotting data demonstrated that Rg3 reduced the expression of extracellular signal-regulated kinase (ERK) and protein kinase B (Akt) *in vitro* and *in vivo*. This result indicated that the antimelanoma effects of Rg3 may be mediated through suppression of ERK and Akt signaling. Further research is required to assess the value of Rg3 as a novel therapeutic strategy for melanoma in the clinical setting.

Correspondence to: Dr Ying Xin, Key Laboratory of Pathobiology, Ministry of Education, Jilin University, 126 Xinmin Street, Changchun, Jilin 130021, P.R. China
E-mail: rji@mail.valenciacollege.edu

Dr Xin Jiang, Department of Radiation Oncology, The First Hospital of Jilin University, 71 Xinmin Street, Changchun, Jilin 130021, P.R. China
E-mail: jiangx@jlu.edu.cn

Abbreviations: ERK, extracellular signal-regulated kinase; PCNA, proliferating cell nuclear antigen; MMP, matrix metalloproteinase; VEGF, vascular endothelial growth factor

Key words: advanced melanoma, proliferating cell nuclear antigen, matrix metalloproteinase, vascular endothelial growth factor, extracellular signal-regulated kinase, protein kinase B, mammalian target of rapamycin

Introduction

Melanoma is a type of skin cancer that develops from melanin-containing cells (melanocytes) located in the basal layer of the epidermis (1). The incidence of melanoma is the lowest among all skin cancers, but it is the most malignant and aggressive type of skin cancer, accounting for 75% of skin cancer-related deaths (2). Advanced melanoma frequently metastasizes to the lymph nodes (stage III) or distant organs (stage IV) (2,3). In 2017, ~87,100 individuals were diagnosed with advanced melanoma and 9,730 succumbed to the disease in the United States (4). At an early stage, melanoma may be curable by surgical excision, with a 5-year survival rate of >95% (5). However, at the advanced or metastatic stage there are fewer treatment options for controlling melanoma progression; as a result, the 5-year survival rate markedly decreases to 16% (6). Over the past decade, a large number of studies and clinical trials have been conducted to assess the potential molecular pathogenesis and treatment strategies for controlling advanced melanoma (7-18). Traditional chemotherapy was first used to inhibit tumor cell division, but with little survival benefit (7). Several intracellular signaling pathways have been identified, such as the mitogen-activated protein kinase (MAPK) (8-10) and phosphatidylinositol 3-kinase (PI3K)/protein kinase B (Akt) pathways (11-13), while a number of mutated oncogenes have also been identified, including BRAF (14,15), c-KIT (16,17) and RAS (18,19). These findings have led to novel approaches to controlling melanoma progression biologically, which have indeed achieved some improvement (20-22). More recently, tumor immunotherapy was applied to treat

metastatic melanoma, such as pembrolizumab and nivolumab, which are programmed cell death protein 1 (PD-1) inhibitors that act by blocking the interaction of PD-1 with PD-L1 and restore immune function to eliminate tumor cells (23-25). Unfortunately, all these therapies have exhibited only limited effectiveness, as tumor resistance eventually develops. Thus, further study of new agents and the molecular mechanisms underlying melanoma development and progression may help identify novel therapeutic targets or drugs for controlling advanced melanoma.

Ginsenoside Rg3, a type of steroidal saponin component, is extracted from steamed *Panax ginseng* and has been shown to promote immune response and possess antitumor activity (26). Rg3 is the most active extract of steroidal saponins (27) and has been shown to inhibit the growth of different types of human cancers, such as colon (28,29), lung (30,31), breast (32), ovarian (33,34) and gallbladder cancers (35), glioma (36,37), leukemia (38) and hepatocellular carcinoma (39,40). Mechanistically, Rg3 was able to induce tumor cell apoptosis, thereby inhibiting tumor cell proliferation and metastasis (28-40) by suppression of nuclear factor (NF)-κB (29,41), AP-1 (activator protein 1) (42), vascular endothelial growth factor (VEGF) (43,44) and PI3K/Akt signaling (33,38), and activation of AMP-activated protein kinase (AMPK) pathway-related apoptosis (45). Considering these antitumor effects, Rg3 warrants further investigation as a novel and promising agent in the treatment of advanced melanoma.

In the present study, the role of Rg3 in melanoma was further assessed by evaluating its *in vitro* and *in vivo* inhibitory effects on melanoma cell growth and metastasis and melanoma-induced angiogenesis, aiming to provide useful insight into the effects of Rg3 on B16 melanoma cells and elucidate the underlying molecular events.

Materials and methods

Animals and cell lines. This animal use protocol was approved by the Animal Care and Use Committee of the Chinese Academy of Medical Sciences. A total of 200, 6-week-old, male C57BL/6 mice (weighing ~21 g) were purchased from Beijing Experimental Animal Technical Co., Ltd., and housed at the Animal Center of Jilin University under the following conditions: Housing, 5 mice per cage; temperature, 22-25˚C; humidity, 50-60%; 12 h light/dark cycle. The mice had access to food and water *ad libitum*.

A highly metastatic subline of murine B16 melanoma cells were kindly provided by Dr Xiaochun Xu of UT M.D. Anderson Cancer Center and cultured in RPMI-1640 medium supplemented with 10% fetal bovine serum (FBS), 1 mM pyruvate, 4 mM L-glutamine, penicillin (100 U/ml) and streptomycin (100 μg/ml), and 100 μg/ml hygromycin B (all from Thermo Fisher Scientific, Inc., Waltham, MA, USA).

Tumor cell viability determination using the MTT assay. To assess the effects of ginsenoside Rg3 on tumor cells *in vitro*, B16 cells were plated in 96-well plates at a density of $4x10^3$ cells/well and incubated overnight, and were then treated for 72 h with a series of concentrations (1, 2.5, 5, 7.5, 10, 12.5 or 15 μg/ml) of Rg3 (Shanghai Haoran Biological Technology Co., Ltd., Shanghai, China). Rg3 was dissolved in dimethyl sulfoxide (DMSO; Sigma-Aldrich; Merck KGaA, Darmstadt, Germany) and filtered through a 0.2-μm membrane before use. At the end of the experiments, cell proliferation was assessed by 10% MTT (Sigma-Aldrich; Merck KGaA), as described previously (46).

Cell counting assay. B16 cells ($1.5x10^4$) were seeded into 24-well plates and grown for 24 h, followed by treatment with different concentrations of Rg3 (2.5, 5 and 7.5 μg/ml) or 1% DMSO (control) for up to 6 days. The cells were then stained with 1% trypan blue (Bio-Rad Laboratories, Inc., Hercules, CA, USA) and the number of living cells was determined using a Bio-Rad TC10 Automated Cell Counter.

Flow cytometric cell cycle distribution assay. After 48 h of treatment with DMSO (control) and 2.5 or 5 μg/ml Rg3, B16 cells were trypsinized, washed with ice-cold phosphate-buffered saline (PBS), and fixed in 70% ethanol overnight. On the following day, the cells were stained with 0.5 mg/ml propidium iodide (PI; Sigma-Aldrich; Merck KGaA) in PBS containing 50 μg/ml RNase A (Sigma-Aldrich; Merck KGaA) and then analyzed using a flow cytometer with ModiFit LT™ software version 4.0 (BD Biosciences, Franklin Lakes, NJ, USA).

Immunofluorescence and immunohistochemistry. B16 cells were plated onto coverslips in 24-well plates at a density of $1x10^5$ cells/well and grown overnight, followed by treatment with 5 μg/ml Rg3 for 24 h. The cells were then fixed with 4% freshly made paraformaldehyde and assessed with immunofluorescence, as described previously (47). A primary antibody against mouse PCNA (BioLegend, Inc., San Diego, CA, USA) and a fluorochrome-conjugated secondary antibody (1:500; Santa Cruz Biotechnology, Inc., Dallas, TX, USA) were used in this study.

B16-formed tumors from animal experiments were fixed in 4% paraformaldehyde solution and embedded in paraffin to prepare 5-µm sections. The tissue sections were then evaluated using immunohistochemistry, as described previously (47). A mouse anti-PCNA (1:500; BioLegend, Inc.) or rat anti-mouse VEGF antibody (1:500, BioLegend, Inc.) was used in the present study.

Tumor cell invasion assay. B16 cells were grown and treated with 0, 2.5 and 5 μg/ml Rg3 for 24 h, and then detached with 0.25% trypsin/EDTA solution (Sigma-Aldrich; Merck KGaA) for 5 min. Following inactivation of trypsin by addition of an equal volume of serum-containing medium, the cells were counted with a hemocytometer and placed into the top wells of Boyden chambers (BD Biosciences) at a density of $2x10^4$, while the filters (8-μm pore size) were pre-coated with Matrigel (65 μl/filter; Osmonics, Inc., Minnetonka, MN, USA; the bottom wells were filled with 20% FBS-containing medium and the cells were incubated for 5 h. Subsequently, cells that had invaded into the lower surface of the filters were fixed with methanol for 10 min, stained with Harris' hematoxylin (Sigma-Aldrich; Merck KGaA) for 10 min, and then counted under an inverted Olympus IMT-2 microscope (Olympus Corporation, Tokyo, Japan) at a magnification of x400. Cell

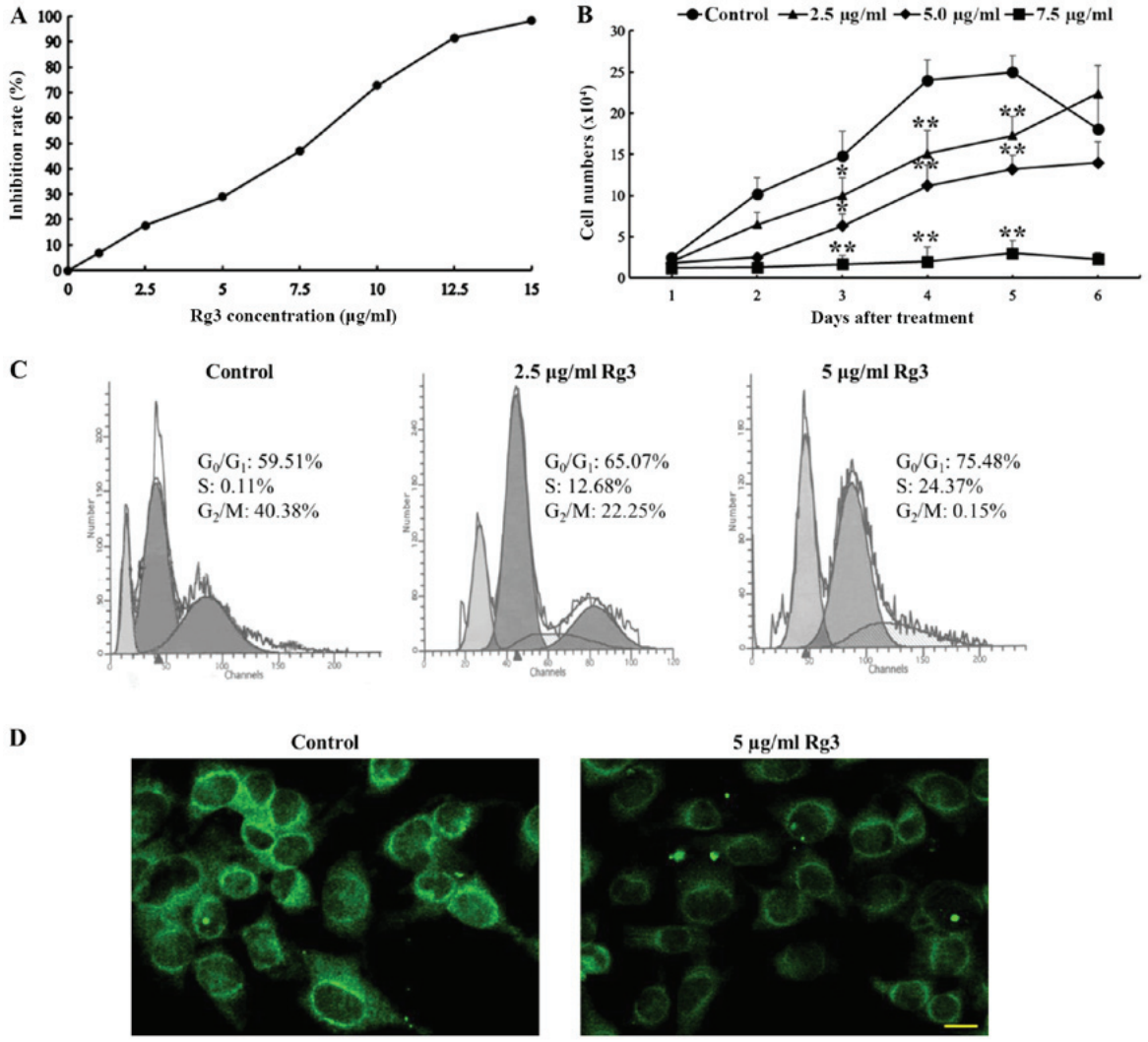

Figure 1. Rg3 inhibition of B16 cell proliferation *in vitro*. (A) The inhibition rate of B16 cell growth was analyzed by the MTT assay. (B) Growth curve of B16 melanoma cells after treatment with 2.5, 5 and 7.5 μg/ml Rg3. Data are presented as mean ± standard deviation. *P<0.05, **P<0.01, n=3. (C) The cell cycle of B16 cells treated with 2.5, 5 and 7.5 μg/ml Rg3 for 48 h was analyzed by flow cytometry. (D) The expression of PCNA in B16 cells after treatment with 5 μg/ml Rg3 was assessed by immunostaining. Scale bar, 10 μm. PCNA, proliferating cell nuclear antigen.

numbers from 18 microscopic fields were summed for each filter.

Vascular endothelial cell proliferation and migration assays. B16 cells were grown in RPMI-1640 medium containing 0 (control) or 5 μg/ml Rg3 for 24 h, and the conditioned medium was used to culture vascular endothelial cells (Cell Bank of Chinese Academy of Sciences, Beijing, China) for an additional 24 h, followed by cell viability MTT assay, PCNA staining and Boyden chamber invasion assay, as described above.

Western blot analysis. B16 cells were grown and treated with 0 (control) or 5 μg/ml Rg3 for 0, 24, 48 or 72 h and lysed for western blotting. Mouse tumor xenografts were also lysed for western blotting. The protocol was performed as described previously (47). Rabbit polyclonal antibodies against ERK (cat. no. sc-514302) and p-ERK (cat. no. sc-13073), Akt (cat. no. sc-8312) and p-Akt (cat. no. sc-7985-R), mammalian target of rapamycin (mTOR) (cat. no. sc-8319) and p-mTOR (cat. no. sc-101738), hypoxia-inducible factor (HIF)-1α (cat. no. sc-10790) and β-actin (cat. no. sc-130656) were used according to the manufacturer's suggested dilutions (all from Santa Cruz Biotechnology, Inc.).

Mouse tumor cell xenograft assay. C57BL/6 mice were subcutaneously injected in the right flank with $2x10^6$ B16 cells, and then randomly divided into five groups (n=10) and intraperitoneally injected with DMSO (control) and 0.3, 1.0 or 3.0 mg/kg Rg3 and/or 20 mg/kg 5-fluorouracil (5-FU; Sigma-Aldrich; Merck KGaA) for 10 consecutive days. Two days after drug withdrawal, the mice were sacrificed and the tumors were resected, weighed and examined for PCNA expression.

Mouse tumor cell metastasis assay. C57BL/6 mice were subcutaneously injected in the right hind footpad with $5x10^5$ B16 cells, and then randomly divided into 5 groups (n=10) and intraperitoneally injected with DMSO (control) and 0.3, 1.0 or 3.0 mg/kg Rg3 and/or 20 mg/kg 5-FU (Sigma-Aldrich; Merck KGaA) for 35 consecutive days. The primary tumors were excised 21 days after the subcutaneous injection of B16 cells. At 14 days after resection, the mice were sacrificed

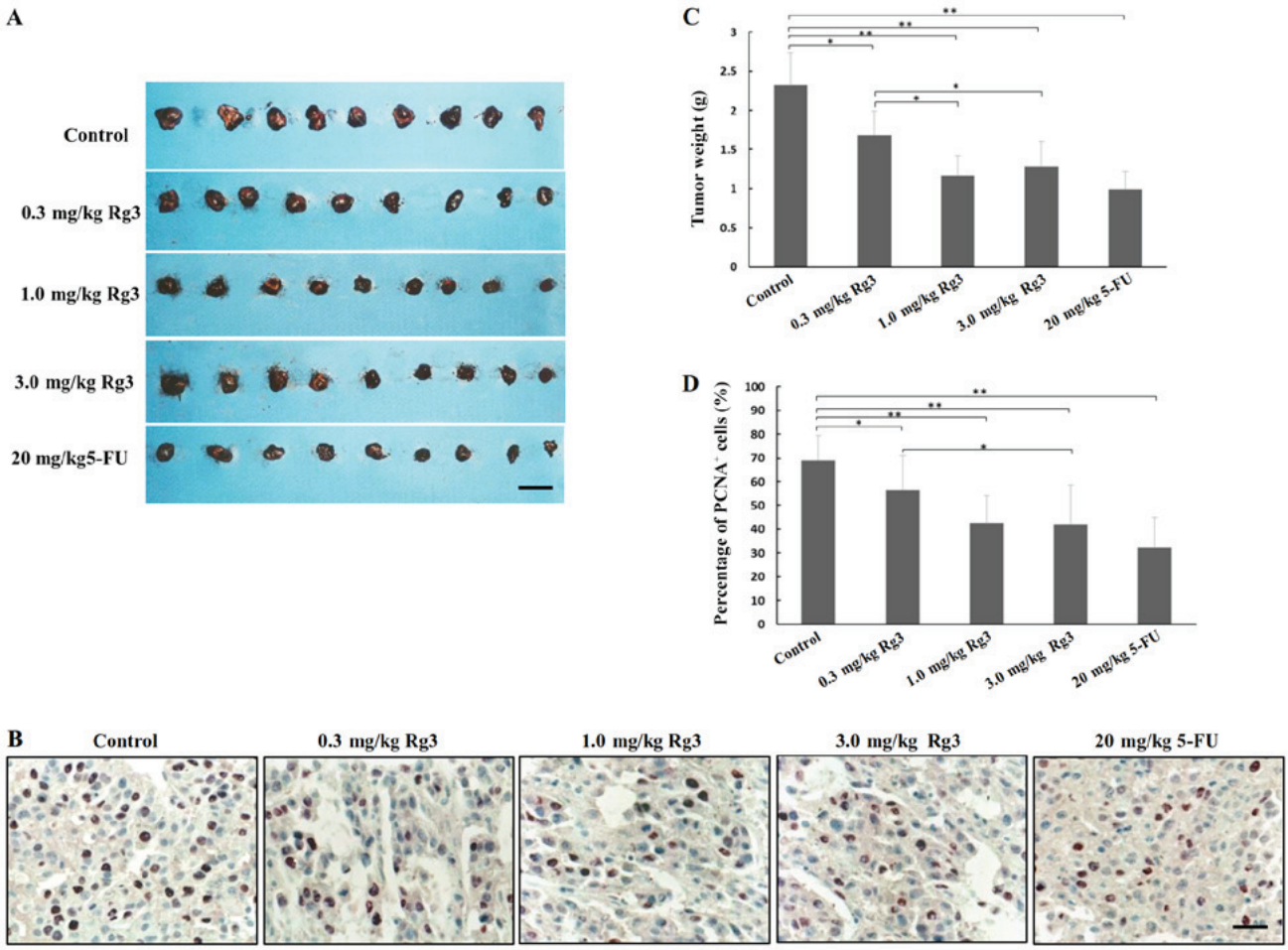

Figure 2. Rg3 inhibition of B16 cell xenograft growth *in vivo*. (A) Macroscopic images of B16 tumors derived from mice treated with 0 (control), 0.3, 1.0 or 3.0 mg/kg Rg3, and 20 mg/kg 5-FU. The largest subcutaneous tumor detected in the present study had a diameter of 1.9 cm. Scale bar, 2 cm. (B) Representative images of PCNA immunohistochemical staining of B16 tumor xenografts (scale bar, 20 μm). (C) Analysis of B16 tumor weight. (D) Percentage of B16 tumor cells exhibiting positive PCNA staining. Data are presented as mean ± standard deviation. *P<0.05, **P<0.01, n=9. PCNA, proliferating cell nuclear antigen; 5-FU, 5-fluorouracil.

and their lungs were fixed in Bouin's solution for analysis of tumor cell metastasis.

B16 cell-induced mouse angiogenesis assay. C57BL/6 mice were inoculated intradermally with $5x10^5$ B16 cells on the dorsal flank flap and then randomly divided into four groups (n=3) and intraperitoneally injected with 0 (control), 0.3, 1.0 or 3.0 mg/kg Rg3 for 5 consecutive days. Seven days after the last injection, the mice were sacrificed and the skin was separated from the underlying tissues for quantification of angiogenesis by counting the number of vessels oriented toward the tumor mass under a dissecting microscope. The tumor size was approximated by averaging the diameters of the short and long axes of the residual inoculated cells.

Determination of microvascular density (MVD). Tumor tissues from the angiogenesis assay were stained with antibodies against the endothelial marker CD31, and MVD was determined according to the method of Weidner *et al* (48).

Statistical analysis. Data are expressed as the mean ± standard deviation and were statistically analyzed using analysis of variance (ANOVA) or the unpaired t-test for two-group comparisons, while the ANOVA Tukey's multiple comparison test was performed for analysis of differences among three or more groups. All experiments were performed in triplicate and repeated at least three times. P≤0.05 was considered to indicate statistically significant differences.

Results

Rg3 inhibits the growth of B16 melanoma cells. In the present study, the effect of Rg3 on the growth of B16 melanoma cells was first evaluated *in vitro*, and Rg3 was found to significantly inhibit B16 cell growth in a dose-dependent manner (Fig. 1A); the IC_{50} was 7.76±0.46 μg/ml. The cell counting assay revealed that Rg3 also reduced the numbers of living B16 melanoma cells in a dose-dependent manner (Fig. 1B). Moreover, the cell cycle analysis demonstrated that 48 h of treatment with Rg3 led to an arrest of the cell cycle at the S phase (0.11 vs. 12.68 and 24.37% after 2.5 and 5 μg/ml of Rg3 treatment, respectively; Fig. 1C). As shown in Fig. 1D, Rg3 significantly downregulated PCNA expression in B16 melanoma cells.

Furthermore, our *in vivo* data on B16 cell xenografts and Rg3 treatment demonstrated that tumor growth (Fig. 2A and C) and PCNA expression (Fig. 2B and D) in Rg3-treated mouse

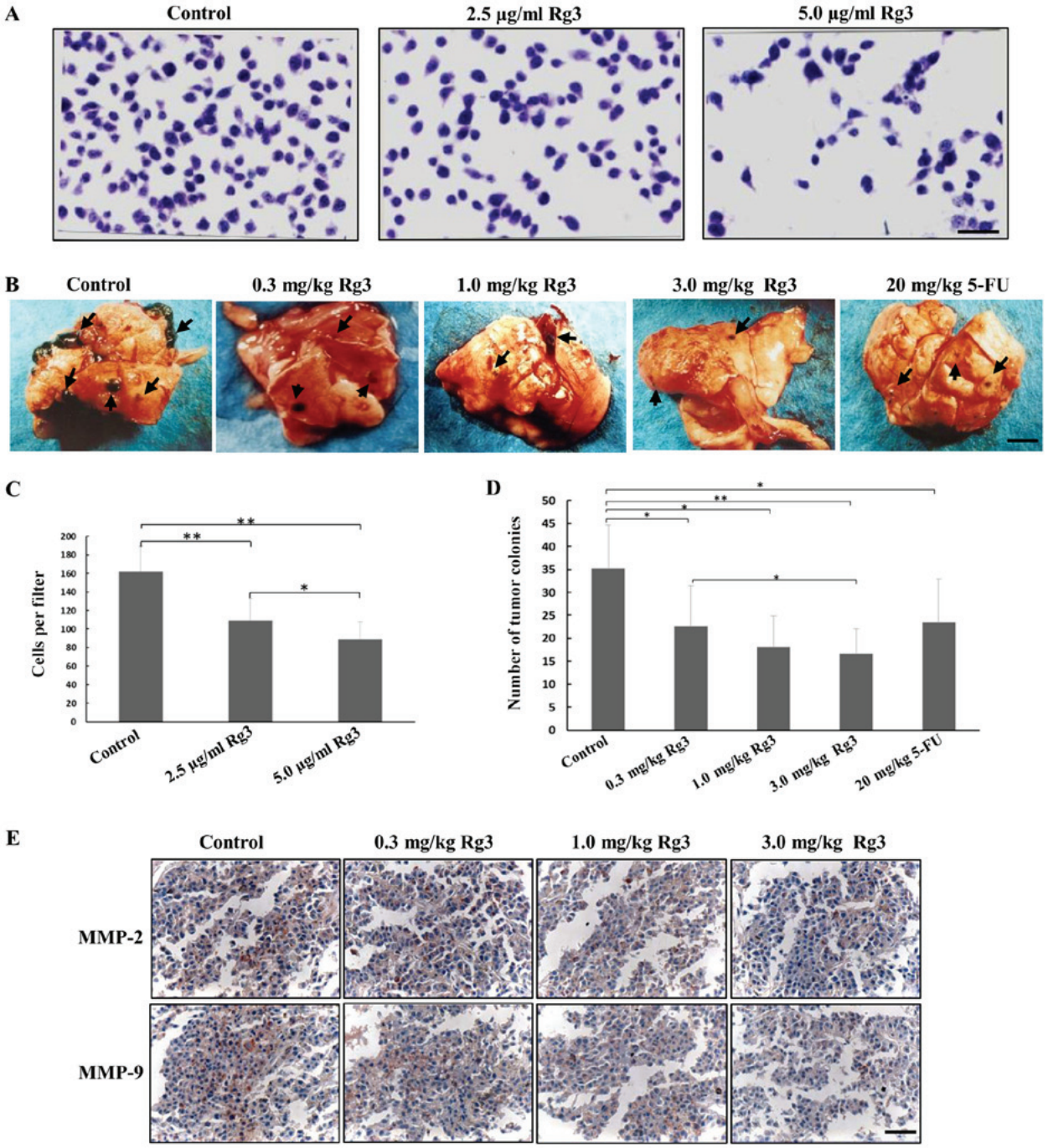

Figure 3. Rg3 inhibition of tumor cell invasion *in vitro* and *in vivo*. (A) Representative images of Boyden chamber assay showing B16 melanoma cell invasion capacity after treatment with 0 (control), 2.5, or 5 μg/ml Rg3. Scale bar, 20 μm. (B) Representative images of lung tissues with B16 tumor colonies from mice treated with intraperitoneal injection of 0, 0.3, 1.0, or 3.0 mg/kg Rg3 and 20 mg/kg 5-FU. Scale bar, 1 cm. (C) Number of B16 cells passing through the filter. (D) Number of tumor colonies in the lung tissues. Data are presented as mean ± standard deviation. *P<0.05, **P<0.01, n=3. (E) Representative images of mouse tumor expression of MMP-2 and -9 after intraperitoneal injection of 0 (control), 0.3, 1.0, or 3.0 mg/kg Rg3. Scale bar, 40 μm. 5-FU, 5-fluorouracil; MMP, matrix metallopeptidase.

tumor cell xenografts were inhibited in a dose-dependent manner (1 or 3 mg/kg Rg3 exerted a stronger inhibitory effect compared with 0.3 mg/kg Rg3, P<0.05; however, there was no significant difference between 1 or 3 mg/kg Rg3 and 20 mg/kg 5-FU).

Rg3 inhibits the metastasis of B16 melanoma cells. We then assessed the effect of Rg3 on tumor cell invasion and metastasis, and found that the *in vitro* invasion capacity of B16 cells treated with 2.5 or 5 μg/ml Rg3 was significantly reduced compared with that of controls (P<0.01; Fig. 3A and C). Trypan blue staining demonstrated similar numbers of living cells among these three groups of cells before being placed into Boyden chambers (data not shown), ruling out the possibility of Rg3 cytotoxicity.

Furthermore, the *in vivo* tumor cell metastasis assay demonstrated that mice injected intraperitoneally with 0.3, 1.0 or 3.0 mg/kg Rg3, or 20 mg/kg 5-FU daily for 7 weeks

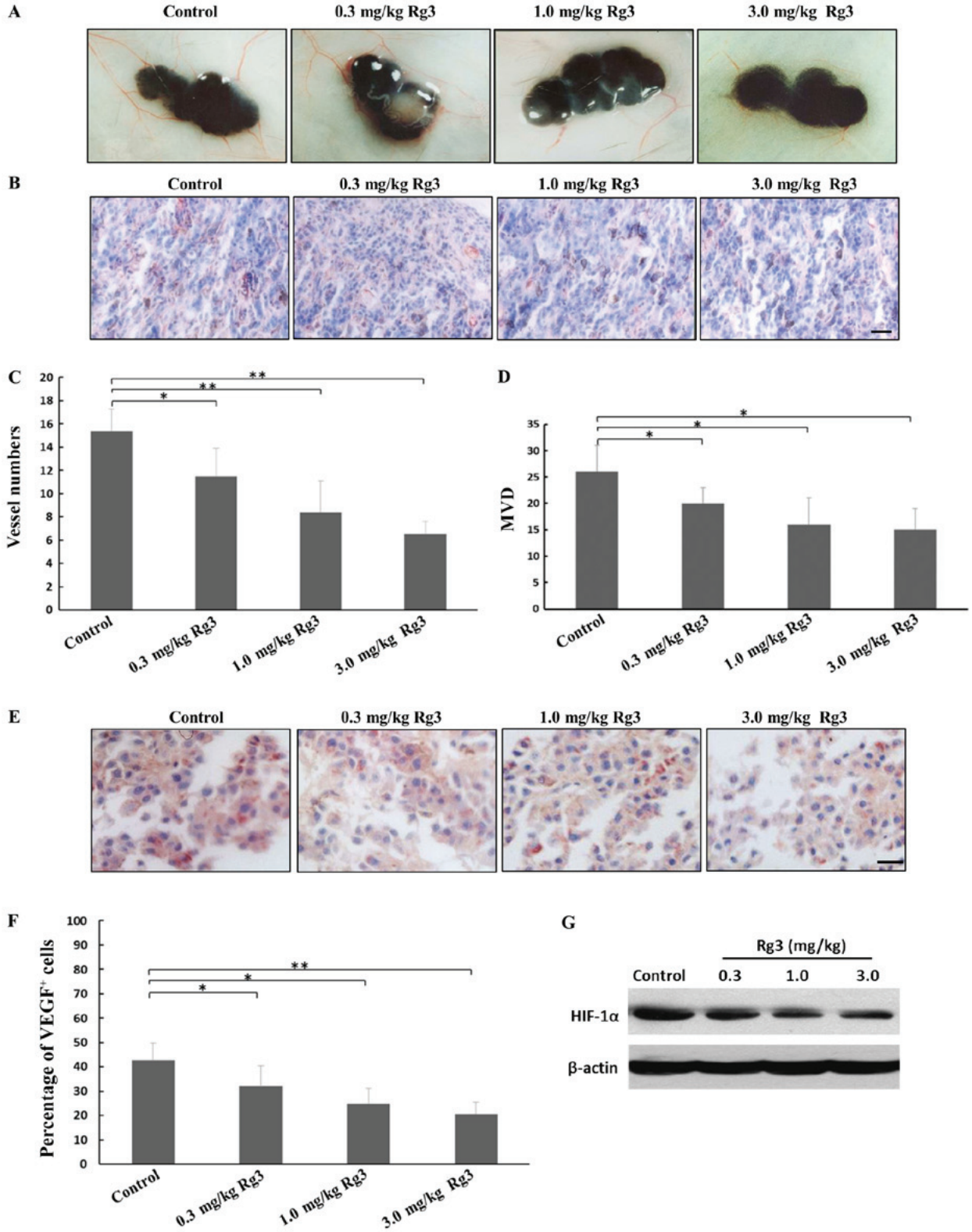

Figure 4. Rg3 inhibition of B16 cell-induced angiogenesis and VEGF expression. (A) Representative images of dermal angiogenesis in mice treated with intraperitoneal injection of 0 (control), 0.3, 1.0, or 3.0 mg/kg Rg3. (B) Representative images of CD31 staining of tumor tissues. Scale bar, 40 μm. (C) Number of vessels oriented toward B16 cells. (D) MVD was determined by counting the number of $CD31^+$ microvessels per high-power field. (E) Representative images of tumor VEGF expression in mice treated with intraperitoneal injection of 0 (control), 0.3, 1.0, or 3.0 mg/kg Rg3. Scale bar, 20 μm. (F) Percentage of tumor cells exhibiting strong VEGF staining. (G) Representative images of western blots showing the levels of HIF-1α and β-actin in tumor xenograft tissues. Data are presented as mean ± standard deviation. $^*P<0.05$, $^{**}P<0.01$, n=3. VEGF, vascular endothelial growth factor; MVD, microvascular density; HIF, hypoxia-inducible factor.

exhibited markedly reduced numbers of lung metastatic nodules (Fig. 3B and D). As the 3.0 mg/kg Rg3 group had a lower number of tumor cell lung metastatic nodules compared with the 0.3 mg/kg Rg3 group ($P<0.05$), the inhibitory

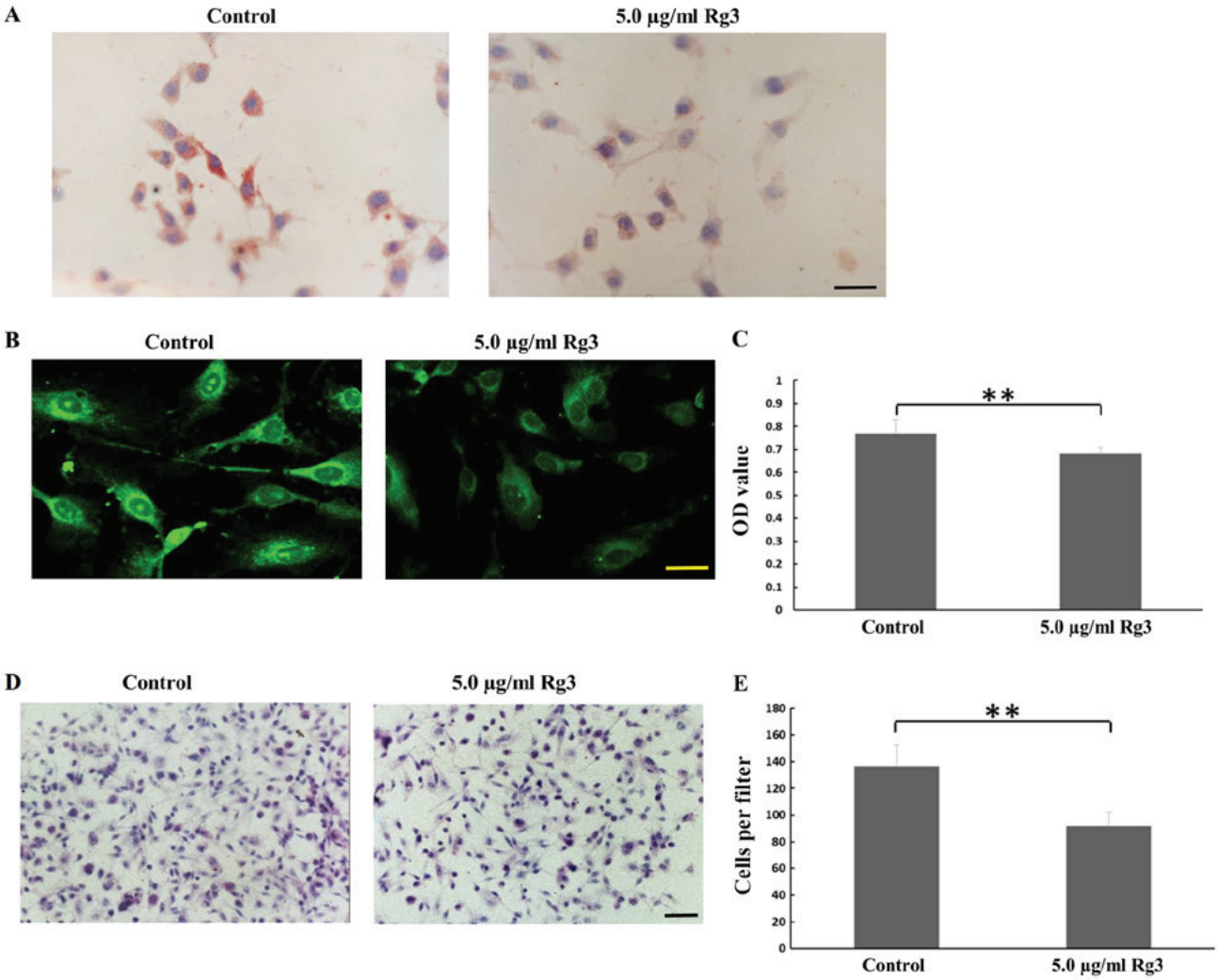

Figure 5. Effects of Rg3-stimulated B16 cell conditioned medium on inhibition of vascular endothelial cell proliferation and migration. (A) Representative images of VEGF staining in B16 cells cultured on coverslips. Scale bar, 20 μm. (B) Representative images of PCNA staining in vascular endothelial cells. Scale bar, 10 μm. (C) OD value from the MTT assay of proliferation of vascular endothelial cells. (D) Representative images of Boyden chamber invasion assay of vascular endothelial cells. Scale bar, 40 μm. (E) Number of endothelial cells passing through the filters. Data are presented as mean ± standard deviation. **P<0.01, n=3. PCNA, proliferating cell nuclear antigen; VEGF, vascular endothelial growth factor; OD, optical density.

effect was dose-dependent. Moreover, since MMP-2 and MMP-9 were highly associated with tumor invasion and metastasis (49,50), their expression was assessed in Rg3-treated tumor tissues using immunohistochemistry and was found to be downregulated (Fig. 3E).

Rg3 inhibits B16 melanoma-induced angiogenesis by reducing VEGF expression. Angiogenesis is an important characteristic of tumor lesions, as melanoma growth and metastasis are dependent on angiogenesis (51). We hereby investigated the effect of Rg3 on B16 melanoma-induced angiogenesis. Seven days after intradermal injection of B16 cells, tumor lesions had formed in the skin and the number of vessels oriented toward the tumor lesions was counted. We found that intraperitoneal injection of Rg3 was associated with a slightly smaller tumor size, but the difference relative to the control was not statistically significant (data not shown). However, the number of blood vessels in the Rg3 groups were markedly reduced compared with the control group (Fig. 4A and C). In addition, CD31 staining revealed that MVD was significantly reduced following treatment with Rg3 (Fig. 4B and D). Since VEGF is a key factor in the regulation of angiogenesis (52), VEGF expression was evaluated in these tumor lesions and was found to be downregulated in Rg3 groups (Fig. 4E and F). Reduced expression of VEGF may be caused by downregulation of the main transcription factor, HIF-1a (Fig. 4G). Furthermore, Rg3 also inhibited the expression of VEGF in B16 cells cultured on coverslips (Fig. 5A) and the effects of B16 cell-conditioned medium on regulation of proliferation and migration of vascular endothelial cells was then assessed. Our data demonstrated that Rg3-treated vascular endothelial cells exhibited weaker staining for PCNA and lower OD value, indicating that Rg3 reduced vascular endothelial cell proliferation (Fig. 5B and C) and migration (Fig. 5D and E).

To summarize, Rg3 inhibited the expression of VEGF in B16 cells, and VEGF downregulation further decreased angiogenesis by attenuating proliferation and migration of vascular endothelial cells.

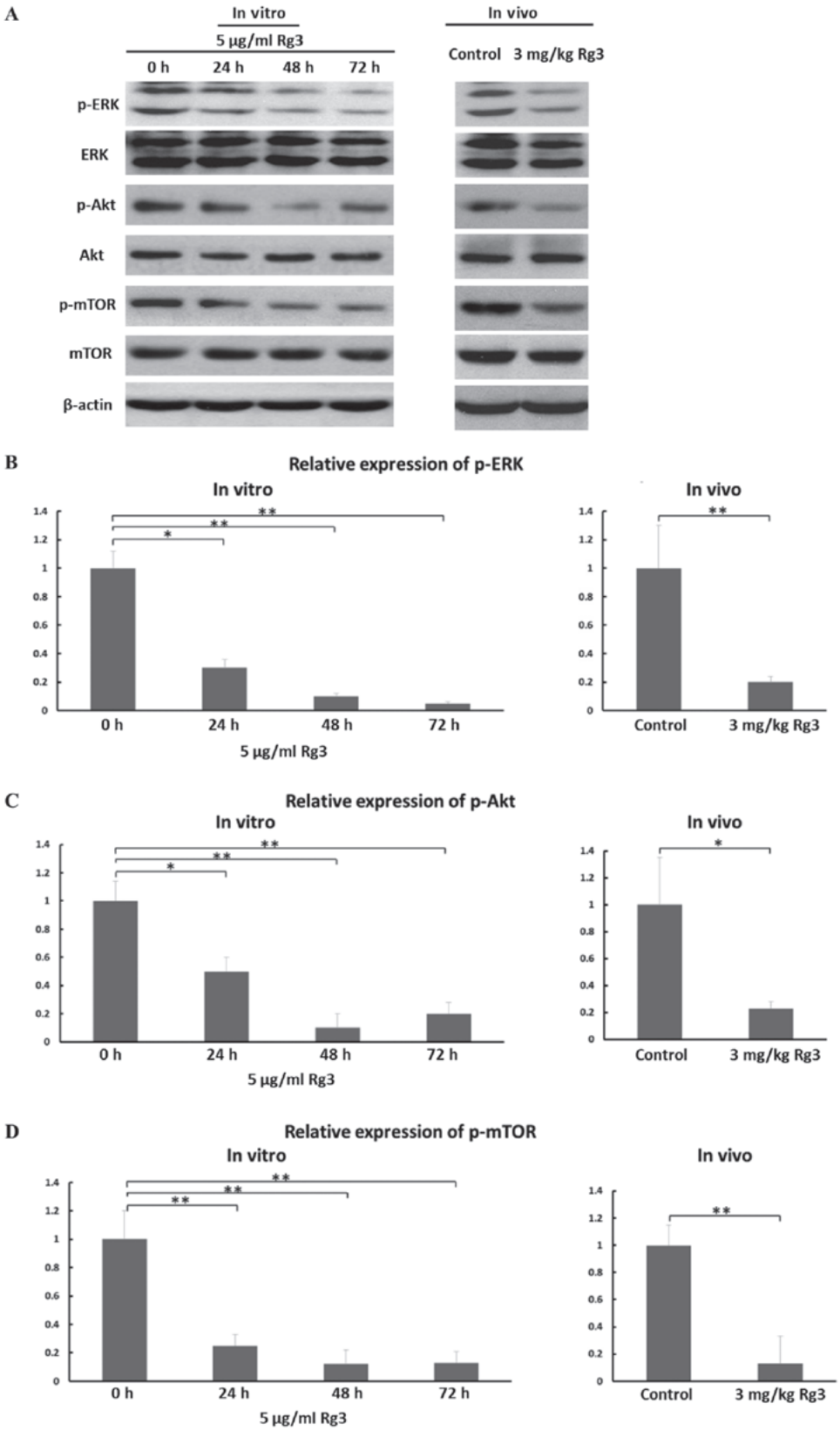

Figure 6. Effects of Rg3 on the regulation of ERK and Akt signaling pathways. (A) Representative images of western blots showing the levels of p-ERK, ERK, p-Akt, Akt, p-mTOR, mTOR and β-actin in B16 cells (*in vitro*) and tumor xenograft tissues (*in vivo*). The cells were incubated with 5 μg/ml Rg3 and mice were treated with 3 mg/kg Rg3. (B) Relative expression of p-ERK in cells and tumor xenograft tissues. (C) Relative expression of p-Akt in cells and tumor xenograft tissues. (D) Relative expression of p-mTOR in cells and tumor xenograft tissues. Data are presented as a mean ± standard deviation. *P<0.05, **P<0.01, n=3. ERK, extracellular signal-regulated kinase; Akt, protein kinase B; mTOR, mammalian target of rapamycin.

The antitumor effects of Rg3 are mediated by regulation of ERK and Akt signaling. Finally, we attempted to explore the molecular pathways underlying the antitumor role of Rg3. Since ERK and Akt signaling are two major pathways

implicated in melanoma progression, the expression of their pathway proteins was assessed in B16 cells and tumor tissues. Our data demonstrated that Rg3 treatment decreased the levels of phosphorylated ERK, Akt and mTOR in B16 cells and tumor cell xenografts (Fig. 6). However, there was no significant change in the expression of total ERK, Akt and mTOR (Fig. 6).

Discussion

Advanced melanoma is difficult to control clinically; thus, it is important to develop novel and effective agents for melanoma patients. Rg3, an extract obtained from *Panax ginseng*, has shown antitumor activity in various types of human cancers (28-40). However, the number of studies investigating its role in melanoma is very limited. It was recently demonstrated that Rg3 can inhibit the proliferation of melanoma cells by decreasing HDAC3 and increasing acetylation of p53 (53). However, there are no more reported data on its role in metastasis, melanoma-induced angiogenesis, or other underlying molecular pathways. The aim of the present study was to investigate the antitumor role of Rg3 in melanoma, and determine whether Rg3 can inhibit melanoma growth, lung metastasis and melanoma-induced angiogenesis *in vitro* and *in vivo*. Our data demonstrated that the antitumor effects of Rg3 in melanoma were mediated through downregulation of the ERK and Akt signaling pathways.

Cell cycle progression comprises a series of events that take place during cell proliferation, including the G_0, G_1, S, G_2 and M phases of the cell cycle (54). Our data revealed that exposure of B16 cells to Rg3 arrested tumor cells at the S phase of the cell cycle. Since DNA is synthesized in the S phase, this result indicates that Rg3 can prevent DNA synthesis in melanoma cells, which was reflected by the reduction of PCNA immunostaining, a marker of DNA replication (55). However, a previous study on gallbladder cancer revealed that Rg3 induced tumor cell cycle arrest at the G_0/G_1 phase, the major checkpoint for cell division or apoptosis (35), indicating that Rg3 may regulate different checkpoints of the cell cycle in different types of tumor cells.

MMPs are a family of enzymes responsible for the degradation of various extracellular matrix components (49). Among the 20 identified MMPs, MMP-2 and MMP-9 are highly associated with tumor dissemination and invasiveness (49,50). Numerous studies have demonstrated that upregulation of these two proteins is closely associated with tumor metastasis (56,57). The findings of the present study indicated that Rg3 may suppress melanoma cell metastasis through downregulation of MMP-2 and MMP-9 (Fig. 3E). Moreover, MMP-2 and MMP-9 have also been shown to stimulate angiogenesis and promote VEGF release (58,59). VEGF is a potent and selective endothelial mitogen, inducing rapid and complete angiogenic response by binding to its receptor (60). Consistent with these findings, our data are, to the best of our knowledge, the first to demonstrate that Rg3 decreased melanoma-induced angiogenesis by inhibiting the expression of VEGF, which may be attributed to the reduced expression of MMP-2 and MMP-9.

The ERK and Akt signaling pathways are constitutively activated in melanoma, and play a key role in melanoma development and progression (11). Various molecules, such as MMP-2, MMP-9 and VEGF, are regulated by these two pathways (59,61). It has been reported that Rg3 inhibits breast cancer cells by deactivating NF-κB signaling, with ERK and Akt serving as the potential upstream targets (62). Pharmacological inhibitors of the two kinases abrogate the antitumor effect of Rg3 (62). Consistent with these data, our study demonstrated that ERK and Akt signaling was deactivated following Rg3 treatment of B16 cells, supporting the antimelanoma role of Rg3. The downregulation of the two pathways may also explain the reduced expression of MMP-2, MMP-9 and VEGF.

However, in addition to the ERK and Akt pathways, other mechanisms must still be investigated to determine whether they could mediate the effects of Rg3 on melanoma cells *in vitro* and *in vivo*. For example, Rg3 has been shown to induce apoptosis in colon cancer cells by activating AMPK signaling (45). It is worth investigating whether Rg3 exerts a similar effect on melanoma. Furthermore, immune response should be examined to assess whether it is activated by Rg3 in melanoma. As reported previously, Rg3 can activate ovalbumin-induced immune response (63), thereby causing tumor cell elimination (64,65). Therefore, it may be hypothesized that Rg3 may also exert antitumor effects by activating the immune system.

In conclusion, Rg3 effectively reduced melanoma cell growth, metastasis and melanoma-induced angiogenesis *in vitro* and *in vivo* through suppression of DNA synthesis and expression of MMP-2, MMP-9 and VEGF. The underlying molecular events may include downregulation of the ERK and Akt pathways. Based on the findings of the present study, Rg3 may be a promising novel agent for the treatment of melanoma. However, the effectiveness of Rg3 must be further assessed in a clinical trial of metastatic melanoma.

Acknowledgements

The authors would like to thank Xuebo Yan (M.D. Anderson Cancer Center, USA) for technical assistance.

Funding

This study was supported in part by grants from the National Science Foundation of China (no. 81570344 to Ying Xin), the Norman Bethne Program of Jilin University (no. 2015203 to Xin Jiang), the Jilin Provincial Science and Technology Foundations (no. 20180414039GH to Ying Xin), and the Health and Family Planning Commission of Jilin Province Foundations (no. 2016Q034 to Ying Xin).

Availability of data and materials

All the data generated or analyzed during the present study are included in this published article.

Authors' contributions

LM, YX, and XJ designed the project and wrote the paper. LM, RJ and XD performed the experiments and generated data. XX reviewed and edited the manuscript. All authors have read and approved the final version of this manuscript.

Ethics approval and consent to participate

The present study was approved by the Ethics Committee of Jilin University. The animal protocol was approved by the Animal Care and Use Committee of the Chinese Academy of Medical Sciences (Beijing, China).

Patient consent for publication

Not applicable.

Competing interests

The authors declare that they have no competing interests.

References

1. Clark WH Jr, Elder DE and Van Horn M: The biologic forms of malignant melanoma. Hum Pathol 17: 443-450, 1986.
2. Freedman DM, Dosemeci M and McGlynn K: Sunlight and mortality from breast, ovarian, colon, prostate, and non-melanoma skin cancer: A composite death certificate based case-control study. Occup Environ Med 59: 257-262, 2002.
3. Balch CM, Gershenwald JE, Soong SJ, Thompson JF, Atkins MB, Byrd DR, Buzaid AC, Cochran AJ, Coit DG, Ding S, *et al*: Final version of 2009 AJCC melanoma staging and classification. J Clin Oncol 27: 6199-6206, 2009.
4. Burke EE and Zager JS: Pharmacokinetic drug evaluation of talimogene laherparepvec for the treatment of advanced melanoma. Expert Opin Drug Metab Toxicol 14: 469-473, 2018.
5. Singh AD, Turell ME and Topham AK: Uveal melanoma: Trends in incidence, treatment, and survival. Ophthalmology 118: 1881-1885, 2011.
6. Balch CM, Buzaid AC, Soong S-J, Atkins MB, Cascinelli N, Coit DG, Fleming ID, Gershenwald JE, Houghton A Jr, Kirkwood JM, *et al*: Final version of the American Joint Committee on Cancer staging system for cutaneous melanoma. J Clin Oncol 19: 3635-3648, 2001.
7. Bhatia S, Tykodi SS and Thompson JA: Treatment of metastatic melanoma: An overview. Oncology (Williston Park) 23: 488-496, 2009.
8. Cerezo M, Tichet M, Abbe P, Ohanna M, Lehraiki A, Rouaud F, Allegra M, Giacchero D, Bahadoran P, Bertolotto C, *et al*: Metformin blocks melanoma invasion and metastasis development in a AMPK/p53-dependent manner. Molecular cancer therapeutics: Mol Cancer Ther 12: 1605-1615, 2013.
9. Kim H-S, Kim M-J, Kim EJ, Yang Y, Lee M-S and Lim J-S: Berberine-induced AMPK activation inhibits the metastatic potential of melanoma cells via reduction of ERK activity and COX-2 protein expression. Biochem Pharmacol 83: 385-394, 2012.
10. Woodard J and Platanias LC: AMP-activated kinase (AMPK)-generated signals in malignant melanoma cell growth and survival. Biochem Biophys Res Commun 398: 135-139, 2010.
11. Meier F, Schittek B, Busch S, Garbe C, Smalley K, Satyamoorthy K, Li G and Herlyn M: The RAS/RAF/MEK/ERK and PI3K/AKT signaling pathways present molecular targets for the effective treatment of advanced melanoma. Front Biosci 10: 2986-3001, 2005.
12. Shimizu T, Tolcher AW, Papadopoulos KP, Beeram M, Rasco DW, Smith LS, Gunn S, Smetzer L, Mays TA, Kaiser B, *et al*: The clinical effect of the dual-targeting strategy involving PI3K/AKT/mTOR and RAS/MEK/ERK pathways in patients with advanced cancer. Clin Cancer Res 18: 2316-2325, 2012.
13. Davies MA: The role of the PI3K-AKT pathway in melanoma. Cancer J 18: 142-147, 2012.
14. Zimmer L, Hillen U, Livingstone E, Lacouture ME, Busam K, Carvajal RD, Egberts F, Hauschild A, Kashani-Sabet M, Goldinger SM, *et al*: Atypical melanocytic proliferations and new primary melanomas in patients with advanced melanoma undergoing selective BRAF inhibition. J Clin Oncol 30: 2375-2383, 2012.
15. Vultur A, Villanueva J and Herlyn M: Targeting BRAF in advanced melanoma: A first step toward manageable disease. Clin Cancer Res 17: 1658-1663, 2011.
16. Montone KT, Elenitsas R and Elder D: Proto-oncogene c-kit expression in malignant melanoma: protein loss with tumor progression. Mod Pathol 10: 939-944, 1997.
17. Carvajal RD, Antonescu CR, Wolchok JD, Chapman PB, Roman RA, Teitcher J, Panageas KS, Busam KJ, Chmielowski B, Lutzky J, *et al*: KIT as a therapeutic target in metastatic melanoma. JAMA 305: 2327-2334, 2011.
18. Dumaz N, Hayward R, Martin J, Ogilvie L, Hedley D, Curtin JA, Bastian BC, Springer C and Marais R: In melanoma, RAS mutations are accompanied by switching signaling from BRAF to CRAF and disrupted cyclic AMP signaling. Cancer Res 66: 9483-9491, 2006.
19. Fernández-Medarde A and Santos E: Ras in cancer and developmental diseases. Genes Cancer 2: 344-358, 2011.
20. Dhomen N and Marais R: BRAF signaling and targeted therapies in melanoma. Hematol Oncol Clin North Am 23: 529-545, 2009.
21. Guo J, Si L, Kong Y, Flaherty KT, Xu X, Zhu Y, Corless CL, Li L, Li H, Sheng X, *et al*: Phase II, open-label, single-arm trial of imatinib mesylate in patients with metastatic melanoma harboring c-Kit mutation or amplification. J Clin Oncol 29: 2904-2909, 2011.
22. Brose MS, Volpe P, Feldman M, Kumar M, Rishi I, Gerrero R, Einhorn E, Herlyn M, Minna J, Nicholson A, *et al*: BRAF and RAS mutations in human lung cancer and melanoma. Cancer Res 62: 6997-7000, 2002.
23. Mahoney KM, Freeman GJ and McDermott DF: The next immune-checkpoint inhibitors: PD-1/PD-L1 blockade in melanoma. Clin Ther 37: 764-782, 2015.
24. Robert C, Ribas A, Wolchok JD, Hodi FS, Hamid O, Kefford R, Weber JS, Joshua AM, Hwu WJ, Gangadhar TC, *et al*: Anti-programmed-death-receptor-1 treatment with pembrolizumab in ipilimumab-refractory advanced melanoma: A randomised dose-comparison cohort of a phase 1 trial. Lancet 384: 1109-1117, 2014.
25. Robert C, Long GV, Brady B, Dutriaux C, Maio M, Mortier L, Hassel JC, Rutkowski P, McNeil C, Kalinka-Warzocha E, *et al*: Nivolumab in previously untreated melanoma without BRAF mutation. N Engl J Med 372: 320-330, 2015.
26. Wu R, Ru Q, Chen L, Ma B and Li C: Stereospecificity of ginsenoside Rg3 in the promotion of cellular immunity in hepatoma H22-bearing mice. J Food Sci 79: H1430-H1435, 2014.
27. Yang LQ, Wang B, Gan H, Fu ST, Zhu XX, Wu ZN, Zhan DW, Gu RL, Dou GF and Meng ZY: Enhanced oral bioavailability and anti-tumour effect of paclitaxel by 20(s)-ginsenoside Rg3 in vivo. Biopharm Drug Dispos 33: 425-436, 2012.
28. Lee SY, Kim GT, Roh SH, Song JS, Kim HJ, Hong SS, Kwon SW and Park JH: Proteomic analysis of the anti-cancer effect of 20S-ginsenoside Rg3 in human colon cancer cell lines. Biosci Biotechnol Biochem 73: 811-816, 2009.
29. Kim SM, Lee SY, Yuk DY, Moon DC, Choi SS, Kim Y, Han SB, Oh KW and Hong JT: Inhibition of NF-kappaB by ginsenoside Rg3 enhances the susceptibility of colon cancer cells to docetaxel. Arch Pharm Res 32: 755-765, 2009.
30. Zheng Y, Zhang L, Lu Q, Wang X, Yu F, Wang X and Lu Q: NGF-induced Tyro3 and Axl function as survival factors for differentiating PC12 cells. Biochem Biophys Res Commun 378: 371-375, 2009.
31. Zhang Q, Kang X and Zhao W: Antiangiogenic effect of low-dose cyclophosphamide combined with ginsenoside Rg3 on Lewis lung carcinoma. Biochem Biophys Res Commun 342: 824-828, 2006.
32. Zhang Q, Kang X, Yang B, Wang J and Yang F: Antiangiogenic effect of capecitabine combined with ginsenoside Rg3 on breast cancer in mice. Cancer Biother Radiopharm 23: 647-653, 2008.
33. Wang J-H, Nao J-F, Zhang M and He P: 20(s)-ginsenoside Rg3 promotes apoptosis in human ovarian cancer HO-8910 cells through PI3K/Akt and XIAP pathways. Tumour Biol 35: 11985-11994, 2014.
34. Liu T, Zhao L, Zhang Y, Chen W, Liu D, Hou H, Ding L and Li X: Ginsenoside 20(S)-Rg3 targets HIF-1α to block hypoxia-induced epithelial-mesenchymal transition in ovarian cancer cells. PLoS One 9: e103887, 2014.
35. Zhang F, Li M, Wu X, Hu Y, Cao Y, Wang X, Xiang S, Li H, Jiang L, Tan Z, *et al*: 20(S)-ginsenoside Rg3 promotes senescence and apoptosis in gallbladder cancer cells via the p53 pathway. Drug Des Devel Ther 9: 3969-3987, 2015.

36. Sin S, Kim SY and Kim SS: Chronic treatment with ginsenoside Rg3 induces Akt-dependent senescence in human glioma cells. Int J Oncol 41: 1669-1674, 2012.
37. Liu G-Y, Bu X, Yan H and Jia WW-G: 20S-protopanaxadiol-induced programmed cell death in glioma cells through caspase-dependent and -independent pathways. J Nat Prod 70: 259-264, 2007.
38. Qiu X-M, Bai X, Jiang H-F, He P and Wang J-H: 20-(s)-ginsenoside Rg3 induces apoptotic cell death in human leukemic U937 and HL-60 cells through PI3K/Akt pathways. Anticancer Drugs 25: 1072-1080, 2014.
39. Lee J-Y, Jung KH, Morgan MJ, Kang YR, Lee HS, Koo GB, Hong SS, Kwon SW and Kim YS: Sensitization of TRAIL-induced cell death by 20(S)-ginsenoside Rg3 via CHOP-mediated DR5 upregulation in human hepatocellular carcinoma cells. Mol Cancer Ther 12: 274-285, 2013.
40. Park H-M, Kim S-J, Kim J-S and Kang H-S: Reactive oxygen species mediated ginsenoside Rg3- and Rh2-induced apoptosis in hepatoma cells through mitochondrial signaling pathways. Food Chem Toxicol 50: 2736-2741, 2012.
41. Keum Y-S, Han SS, Chun K-S, Park KK, Park JH, Lee SK and Surh YJ: Inhibitory effects of the ginsenoside Rg3 on phorbol ester-induced cyclooxygenase-2 expression, NF-kappaB activation and tumor promotion. Mutat Res 523-524: 75-85, 2003.
42. Kang L-J, Choi Y-J and Lee S-G: Stimulation of TRAF6/TAK1 degradation and inhibition of JNK/AP-1 signalling by ginsenoside Rg3 attenuates hepatitis B virus replication. Int J Biochem Cell Biol 45: 2612-2621, 2013.
43. Liu T-G, Huang Y, Cui D-D, Huang XB, Mao SH, Ji LL, Song HB and Yi C: Inhibitory effect of ginsenoside Rg3 combined with gemcitabine on angiogenesis and growth of lung cancer in mice. BMC Cancer 9: 250, 2009.
44. Kim J-W, Jung S-Y, Kwon Y-H, Lee JH, Lee YM, Lee BY and Kwon SM: Ginsenoside Rg3 attenuates tumor angiogenesis via inhibiting bioactivities of endothelial progenitor cells. Cancer Biol Ther 13: 504-515, 2012.
45. Yuan HD, Quan H-Y, Zhang Y, Kim SH and Chung SH: 20(S)-Ginsenoside Rg3-induced apoptosis in HT-29 colon cancer cells is associated with AMPK signaling pathway. Mol Med Rep 3: 825-831, 2010.
46. Covington KR, Brusco L, Barone I, Tsimelzon A, Selever J, Corona-Rodriguez A, Brown P, Kumar R, Hilsenbeck SG and Fuqua SA: Metastasis tumor-associated protein 2 enhances metastatic behavior and is associated with poor outcomes in estrogen receptor-negative breast cancer. Breast Cancer Res Treat 141: 375-384, 2013.
47. Ji R, Tian S, Lu HJ, Lu Q, Zheng Y, Wang X, Ding J, Li Q and Lu Q: TAM receptors affect adult brain neurogenesis by negative regulation of microglial cell activation. J Immunol 191: 6165-6177, 2013.
48. Weidner N, Semple JP, Welch WR and Folkman J: Tumor angiogenesis and metastasis - correlation in invasive breast carcinoma. N Engl J Med 324: 1-8, 1991.
49. Wieczorek E, Jablonska E, Wasowicz W and Reszka E: Matrix metalloproteinases and genetic mouse models in cancer research: A mini-review. Tumour Biol 36: 163-175, 2015.
50. Foda HD and Zucker S: Matrix metalloproteinases in cancer invasion, metastasis and angiogenesis. Drug Discov Today 6: 478-482, 2001.
51. Folkman J: Role of angiogenesis in tumor growth and metastasis. Semin Oncol 29 (Suppl 16): 15-18, 2002.
52. Carmeliet P: VEGF as a key mediator of angiogenesis in cancer. Oncology 69 (Suppl 3): 4-10, 2005.
53. Shan X, Fu Y-S, Aziz F, Wang X-Q, Yan Q and Liu J-W: Ginsenoside Rg3 inhibits melanoma cell proliferation through down-regulation of histone deacetylase 3 (HDAC3) and increase of p53 acetylation. PLoS One 9: e115401, 2014.
54. Molinari M: Cell cycle checkpoints and their inactivation in human cancer. Cell Prolif 33: 261-274, 2000.
55. Waga S, Hannon GJ, Beach D and Stillman B: The p21 inhibitor of cyclin-dependent kinases controls DNA replication by interaction with PCNA. Nature 369: 574-578, 1994.
56. Deryugina EI and Quigley JP: Matrix metalloproteinases and tumor metastasis. Cancer Metastasis Rev 25: 9-34, 2006.
57. John A and Tuszynski G: The role of matrix metalloproteinases in tumor angiogenesis and tumor metastasis. Pathol Oncol Res 7: 14-23, 2001.
58. Zheng H, Takahashi H, Murai Y, Cui Z, Nomoto K, Niwa H, Tsuneyama K and Takano Y: Expressions of MMP-2, MMP-9 and VEGF are closely linked to growth, invasion, metastasis and angiogenesis of gastric carcinoma. Anticancer Res 26A: 3579-3583, 2006.
59. Adya R, Tan BK, Punn A, Chen J and Randeva HS: Visfatin induces human endothelial VEGF and MMP-2/9 production via MAPK and PI3K/Akt signalling pathways: Novel insights into visfatin-induced angiogenesis. Cardiovasc Res 78: 356-365, 2008.
60. Ferrara N: VEGF and the quest for tumour angiogenesis factors. Nat Rev Cancer 2: 795-803, 2002.
61. Bauvois B: New facets of matrix metalloproteinases MMP-2 and MMP-9 as cell surface transducers: Outside-in signaling and relationship to tumor progression. Biochim Biophys Acta 1825: 29-36, 2012.
62. Kim B-M, Kim D-H, Park J-H, Surh Y-J and Na H-K: Ginsenoside Rg3 inhibits constitutive activation of NF-κB signaling in human breast cancer (MDA-MB-231) cells: ERK and Akt as potential upstream targets. J Cancer Prev 19: 23-30, 2014.
63. Wei X, Chen J, Su F, Su X, Hu T and Hu S: Stereospecificity of ginsenoside Rg3 in promotion of the immune response to ovalbumin in mice. Int Immunol 24: 465-471, 2012.
64. Janeway CA, Travers P, Walport M and Shlomchik MJ: Manipulation of the Immune Response. In: Immunobiology: the immune system in health and disease. 6th edition. Garland Science, New York, NY, pp665-706, 2005.
65. Ribas A, Dummer R, Puzanov I,, VanderWalde A, AndtbackaRHI, Michielin O, Olszanski AJ, Malvehy J, Cebon J, Fernandez E, *et al*: Oncolytic virotherapy promotes intratumoral T cell infiltration and improves anti-PD-1 immunotherapy. Cell 170: 1109-1119. e1110, 2017.

This work is licensed under a Creative Commons Attribution-NonCommercial-NoDerivatives 4.0 International (CC BY-NC-ND 4.0) License.